Circular Dichroism Spectroscopy of Monoclonal Antibodies That Bind a Superpotent Guanidinium Sweetener Ligand†

Sergey Y. Tetin and D. Scott Linthicum*

Department of Biochemistry and Biophysics, Texas A&M University, College Station, Texas 77843

Received July 12, 1995; Revised Manuscript Received November 2, 1995⊗

ABSTRACT: Three monoclonal antibodies (mAb) with nanomolar affinity to the superpotent trisubstituted guanidinium sweetener ligand *N*-(*p*-cyanophenyl)-*N*′-(diphenylmethyl)guanidineacetic acid were studied by circular dichroism (CD) spectroscopy. Two mAb, NC6.8 (IgG2b,κ) and NC10.8 (IgG3,κ), exhibited similar CD spectra, but mAb NC10.14 (IgG2b,λ) had very different CD spectra in both far- and near-UV regions. Some of these differences may be due to effects of aromatic amino acid side chains, especially Trp and Tyr, located at the immunoglobulin intradomain surfaces. Heavy- and light-chain dissociation of reduced Fab fragments in 1 M acetic acid minimized these effects. Ligand binding changed the sign and amplitudes of the near-UV CD spectra of all three mAb. Calculation of the CD difference spectra (bound minus free) of stoichiometrically bound antibody−ligand complexes allowed us to visualize the net spectral changes. On the basis of the three-dimensional structures experimentally solved for NC6.8 and theoretical models of NC10.8 and NC10.14, we suggest that the *p*-cyanophenyl moiety on the sweetener ligand acts as a molecular pointer in the CD spectra and identifies contact aromatic residues in the different antibody binding pockets.

Recent progress in the development of antibody *in vitro* expression systems, site-directed mutagenesis, and recombinant techniques for construction of variable-region fragments (Fv)[1] has revived interest in the problems of structural analyses of immunoglobulins (Ig). Although optical activity-based spectroscopy is a traditional and powerful approach for investigation of protein structures in solution, a number of interesting biophysical problems in the analyses of Ig structures by optical rotatory dispersion (ORD) or circular dichroism (CD) were identified in early works (Dorrington & Tanford, 1970; Jirgensons, 1969). These problems include: (1) a lower than expected amplitude for the far-UV CD spectra considering the high degree of antiparallel β-structure in the Ig molecule; (2) the lack of additivity when the CD spectra of Ig, their isolated heavy (H) and light (L) chains, and proteolytic fragments are calculated using traditional units of mean residue ellipticity; and (3) the appearance of new bands in the CD spectra upon complexation of the antibody with antigen.

Three-dimensional structures for a variety of antibody Fab fragments and single-chain Fv molecules have been solved by X-ray diffraction methods, including structures in the uncomplexed and antigen-complexed forms [for a review, see Padlan (1994)]. This progress has created a structural basis to explain some of the CD spectral features of antibodies and their immune complexes. For example, CD studies of the anti-fluorescein monoclonal antibody (mAb) 4-4-20 suggested that the aromatic amino acid side chains were responsible for the "unusual" parameters of the UV CD spectra (Tetin et al., 1992). These spectral features are due to the particular arrangement of Tyr and Trp residues throughout the 4-4-20 antibody molecule, but much of the effect is localized to the variable (V) regions and the binding site aromatic residues known to be in contact with the fluorescein hapten. These spectroscopic observations were found to be in agreement with the X-ray diffraction analysis of the 4-4-20 Fab−fluorescein complex (Herron et al., 1989).

In an effort to study ligand specificity of the putative sweet taste receptor or binding site, we produced a collection of specific mAb that have nanomolar binding affinity for a superpotent sweet tasting guanidinium ligand (Anchin & Linthicum, 1993). Some of these mAb have sweetener ligand binding profiles that correlate with ligand sweetness, thereby mimicking some of the ligand recognition features of the putative binding site (Droupadi & Linthicum, 1995). The ligand used in these studies, *N*-(*p*-cyanophenyl)-*N*′-(diphenylmethyl)guanidineacetic acid, is more than 200 000 times sweeter than sucrose in a taste threshold test (Muller et al., 1992). The Fab from several of the mAb in our collection have been successfully crystallized, and three-dimensional structures of two of them, mAb NC6.8 (Guddat et al., 1994) and NC10.14 (L. Gudatt et al., in preparation), have been solved at high resolution in the uncomplexed and ligand-complexed forms. In the study presented herein, we examine the UV CD spectra for three antisweetener mAb and demonstrate the participation of aromatic residues in the ligand recognition. The appearance of new CD bands in the near-UV region for the ligand-complexed mAb indicates a specific geometric arrangement of the ligand and the binding site aromatic residues. These CD observations are consistent with the X-ray diffraction studies of the ligand−Fab complexes. In addition, we show that aromatic−aromatic contacts at the interdomain surfaces are essential

† This work was supported by a grant from the National Institutes of Health (GM46535).

⊗ Abstract published in *Advance ACS Abstracts,* January 15, 1996.

[1] Abbreviations: CD, circular dichroism; CDR, complementarity determining region; Fab, antigen binding fragment of Ig; Fv, fragment variable of Ig; H-chain, heavy chain of Ig; Ig, immunoglobulin; L-chain, light chain of Ig; mAb, monoclonal antibody; ORD, optical rotatory dispersion; PBS, phosphate-buffered saline; V-region, variable region of Ig.

0006-2960/96/0435-1258$12.00/0

in the origination of CD spectra for both the near- and far-UV region.

MATERIALS AND METHODS

Monoclonal Antibodies (mAb). Mouse hybridomas producing monoclonal antibodies NC6.8 (IgG2b,κ), NC10.8 (IgG3,κ), and NC10.14 (IgG2b,λ) to the trisubstituted guanidinium sweetener *N*-(*p*-cyanophenyl)-*N*′-(diphenylmethyl)-guanidineacetic acid were previously produced in our laboratory (Anchin & Linthicum, 1993). Variable region amino acid sequences for each mAb were determined by cDNA cloning and sequencing, and are deposited in the GenBank Database (Accession Numbers L23193, L23194, L23187, L23188, L23185, L23186). The Kabat numbering system of L- and H-chain amino acid positions is used in this study (Kabat et al., 1991).

Ascites fluids containing the mAb were produced in mice, and 0.25 mL of 5% dextran sulfate solution was added per 10 mL of ascites fluid. After a 10 min incubation at RT, the resulting dextran−lipoprotein complex was precipitated with 0.9 mL of 0.1 M $CaCl_2$ and removed by centrifugation. The enriched Ig fraction was precipitated with ammonium sulfate (50% of saturation) overnight at 4 °C. IgG purification was achieved with a protein G−Sepharose 4 Fast Flow (Pharmacia−LKB Biotechnology AB, Uppsala, Sweden) affinity column using standard procedures.

The hybridoma cell line 4-4-20 (anti-fluorescein) was kindly provided by Dr. D. M. Kranz (University of Illinois at Urbana−Champaign); this mAb (IgG2a,κ) was precipitated from ascites fluid as above, with a final affinity purification using a fluorescein−ECH Sepharose 4B column, as previously described (Kranz & Voss, 1981).

Fab fragments of all three anti-sweetener mAb were prepared by papain proteolysis and purified by Dr. Lin Shan at the Harrington Cancer Center (Amarillo, TX) as published previously (Guddat et al., 1994). Additional preparations of NC10.14 and Fab 4-4-20 were produced by us using a limited papain proteolysis (papain:IgG ratio of 1:100, w/w) of parent IgG in 50 mM Tris buffer, pH 7.6, containing 150 mM NaCl, 2 mM EDTA, and 1 mM DTT. The time of proteolysis ranged from 3 to 10 min at 37 °C and was optimized for each mAb. The proteolysis was terminated by the addition of iodoacetamide (final concentration 1 mM). For mAb NC10.14, undigested IgG and Fc fragments were removed by absorption using protein A−Sepharose 4B. Fab fragments of mAb 4-4-20 were purified on a fluorescein−ECH Sepharose 4B column, followed by removal of uncleaved IgG using a protein A−Sepharose 4B column.

Mild reductive cleavage of the single interchain disulfide bond in Fab fragments (between the L- and H-chain cysteines at positions L:214 and H:128, respectively) was performed according to the procedures described by Fleishman et al. (1964). After 1 h incubation with 10 mM dithiothreitol (DTT) in 200 mM Tris buffer, pH 8.2, at RT, iodoacetamide (15 mM) was added to block reduced sulfhydryl groups. The proteins were then dialyzed against PBS to obtain Fab fragments with reduced interchain disulfide bonds or dialyzed against ice-cold 1 M acetic acid to dissociate the L- and H-chains. To achieve noncovalent reassociation to produce Fab-like molecules, the dissociated chains in 1 M acetic acid were slowly dialyzed against PBS. A slight precipitate was formed and eliminated by centrifugation. The yield of the protein after this procedure measured by UV absorption (240−350 nm range) was better than 90%. Reassembled Fab fragments showed a single band in 15% polyacrylamide gel electrophoresis in the absence of SDS, indicating that there was complete reassociation.

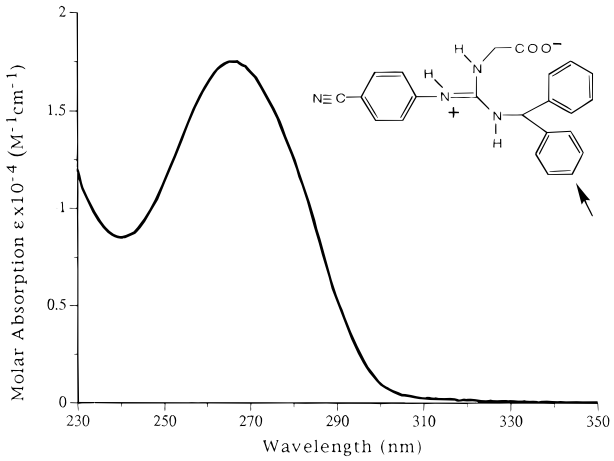

FIGURE 1: Absorption spectrum and chemical structure for the ligand *N*-(*p*-cyanophenyl)-*N*′-(diphenylmethyl)guanidineactic acid. This ligand has a potency of more than 200 000 times that of sucrose as assessed by a threshold taste test for sweetness. The aryl nitrogen (adjacent to the *p*-cyanophenyl) has a pK_a of 9.3, thereby making the ligand a zwitterion at physiological pH. The delocalized positive charge is spread over all three nitrogens and the central guanidine carbon. The arrow indicates the position of hapten conjugation to the carrier protein for the immunogen preparation. The absorption spectrum is recorded in PBS, pH 7.4.

Purities of all Ig and Fab samples were confirmed by electrophoresis using a 15% polyacrylamide gel with 0.1% sodium dodecyl sulfate in reducing and/or nonreducing conditions; the gels showed the reduction and alkylation of Fab fragments used for H- and L-chain reassociation experiments were complete.

Ig and Fab concentrations were determined from absorption spectra. The spectra were recorded in the range 240−400 nm using a Beckman DU 650 spectrophotometer; values were corrected for light scattering with the DU 650 software. The extinction coefficients ($E_{278}^{1\text{mg/mL}}$) were calculated from the amino acid composition of each protein (Mach et al., 1992).

Ligand and Other Reagents. The trisubstituted guanidinium sweetener (Figure 1), *N*-(*p*-cyanophenyl)-*N*′-(diphenylmethyl)guanidineacetic acid (HPLC and MS analytically pure), was a gift provided by the NutraSweet Co. (Mt. Prospect, IL). Initially, the stock ligand solution was prepared by dissolving analytically weighed material in *N*,*N*′-dimethylformamide. The working solutions of the ligand were made by 1000-fold dilution of aliquots from the stock using buffered saline solution (0.15 M NaCl, 0.01 M sodium phosphate buffer, pH 7.4) (PBS). The concentration of the ligand was verified by recording its absorption spectrum in the range of 230−350 nm. The molar extinction coefficient, $\epsilon^M = 17\,800$, was determined in previous analytical experiments; the peak in the absorption spectrum of the ligand recorded in PBS was 265 nm (Figure 1). Organic reagents were obtained from Sigma Chemical Co. (St. Louis, MO); all salts were obtained from FisherBiotech (Fair Lawn, NJ).

Circular Dichroism (CD) Spectra. CD spectra were obtained using a Jasco-710 instrument (Jasco Instruments, Inc., Japan). The calibration of the instrument was performed

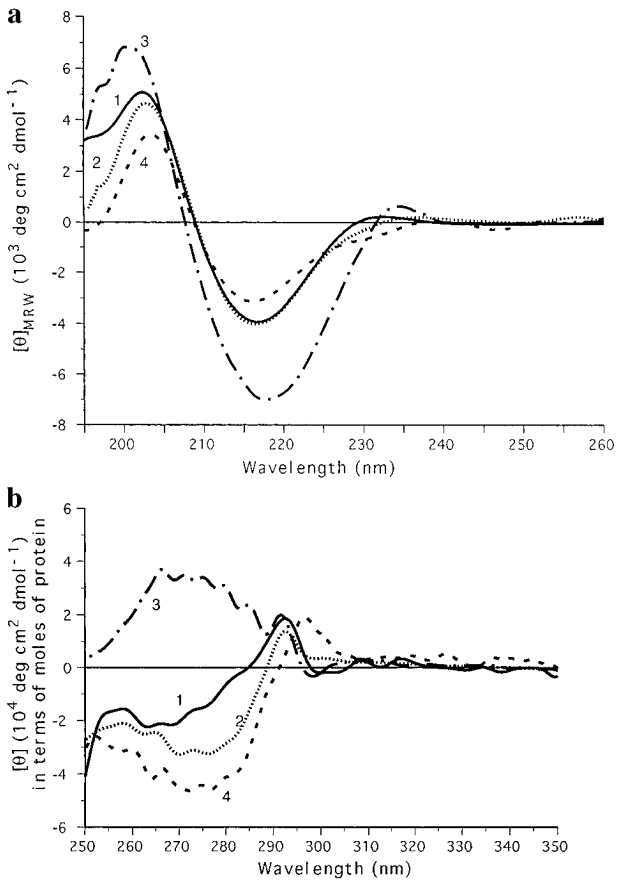

FIGURE 2: (a) Far-UV CD spectra of uncomplexed Fab fragments derived from mAb: NC6.8 (spectrum 1); NC10.8 (2); NC10.14 (3); 4-4-20 (4). (b) Near-UV CD spectra of uncomplexed Fab fragments derived from mAb: NC6.8 (spectrum 1); NC10.8 (2); NC10.14 (3); 4-4-20 (4). All spectra recorded in PBS, pH 7.4.

with a standard solution of (+)-10-camphorsulfonic acid. Each spectrum was measured 5−10 times, recalculated in standard units, and smoothed using Jasco-700 software (version 1.10). Repeated recordings of spectra in the far-UV region using different path length cylindrical cuvettes (0.01, 0.02, and 0.1 cm) allowed us to optimize the signal to noise ratio throughout the spectral regions examined. All spectra were recorded at room temperature. All protein and ligand samples used for spectral measurements were filtered through 0.22-μm Acrodisc low protein binding filters (Gelman Sciences, Ann Arbor, MI).

RESULTS

Uncomplexed Fab Fragments. Figure 2a shows the far-UV CD spectra of uncomplexed Fab fragments derived from the mAb NC6.8, NC10.8, and NC10.14. The results shown are expressed in terms of mean residue weight ellipticity. For comparison, the CD spectrum of the Fab fragment from anti-fluorescein mAb 4-4-20 is also shown; this mAb has been previously studied in detail (Tetin et al., 1992). Two Fab fragments, NC6.8 and NC10.8, exhibited very similar CD spectra in the 195−260 nm region. The CD spectrum of Fab 4-4-20 had the same positions of negative (217 nm) and positive (203 nm) extremes, but proportionally lower amplitudes. All three spectra intersect the zero line at 209 nm. Some minor differences were observed in the region around 230 nm. The CD spectrum of Fab NC10.14, however, was significantly different from the CD spectra of other mAb Fab fragments examined. The amplitude was approximately 2 times higher, and the peaks were slightly shifted. In addition, the Fab NC10.14 CD spectrum showed a small, but very reproducible positive maximum at 233 nm.

Aromatic amino acid side chain chromophores are responsible for the near-UV CD spectra of most proteins. The entire Ig molecule, and especially the Fab regions, contains significant numbers of Trp and Tyr residues (Padlan, 1990, 1994). A previously published investigation of the anti-fluorescein antibody mAb 4-4-20 revealed the majority of the contributions to the CD spectra in the 250−300 nm regions were from aromatic amino acid side chains located in the variable domains. It has been shown (Tetin et al., 1992) that an optimal method for comparison of CD spectra for different antibodies in this spectral region is to express all of the spectra in terms of molar ellipticity calculated based on the molar concentration of the antibody variable portion (V_L and V_H). In the case of Fab fragments, this would be equal to normalization by the molar concentration of the entire protein (each Fab fragment contains only one pair of V domains). All our results of the near-UV CD presented here are calculated according to this procedure.

The near-UV CD spectra of Fab fragments of mAb NC6.8 and NC10.8 were found to be very similar (Figure 2b). The positive maximum was at 291 nm, and the negative broad shoulder, with the maximal amplitude around 270 nm, was characteristic of both mAb. The CD spectrum of Fab 4-4-20 had the same shape, but the position of the positive maximum was shifted to 295 nm, and the negative portion of the spectrum was more pronounced. All spectra were found to intersect the zero line in the region of 285−290 nm. In contrast, Fab of mAb NC10.14 showed only a positive CD spectrum in the near-UV. The overall magnitude and the shape of the NC10.14 spectrum were comparable with the spectra of NC6.8, NC10.8, and 4-4-20, but the broad portion of the spectrum at 250−285 nm was positive in sign.

Reduced, Dissociated, and Reassociated Fab Fragments. Most of the Tyr and Trp residues in the variable domains of mAb NC6.8 and NC10.14 are located at the L- and H-chain interfaces and are similar to the location of the aromatic residues found in the anti-fluorescein mAb 4-4-20 (Tetin et al., 1992). To examine the role of these residues in the origin of the CD spectra, we studied native and reduced Fab, dissociated Fab, and reassociated Fab-like fragments (such fragments can reassociate via L- and H-chain interactions without the stabilizing benefit of the interchain disulfide bond).

Two different mAb fragments, one with a small amplitude (mAb 4-4-20) and the other with a high amplitude (mAb NC10.14) of CD spectra in the far-UV region, and both with very different near-UV CD spectra, were chosen for these experiments. As shown in Figures 3a and 4a, the far-UV CD spectra of both mAb Fab fragments did not change after the mild reduction procedure (compare with Figure 2a). The near-UV CD spectra for both mAb (Figures 3b and 4b) were found also to be unchanged for the reduced Fab forms (compared with Figure 2b). In contrast, dissociation of the L- and H-chains for either mAb Fab by dialysis against 1 M acetic acid significantly altered their CD spectra (Figures 3a and 4a). Dissociated L- and H-chains of Fab NC10.14 showed a broad negative spectrum, with approximately equal amplitudes at 202 and 217 nm. Dissociated L- and H-chains

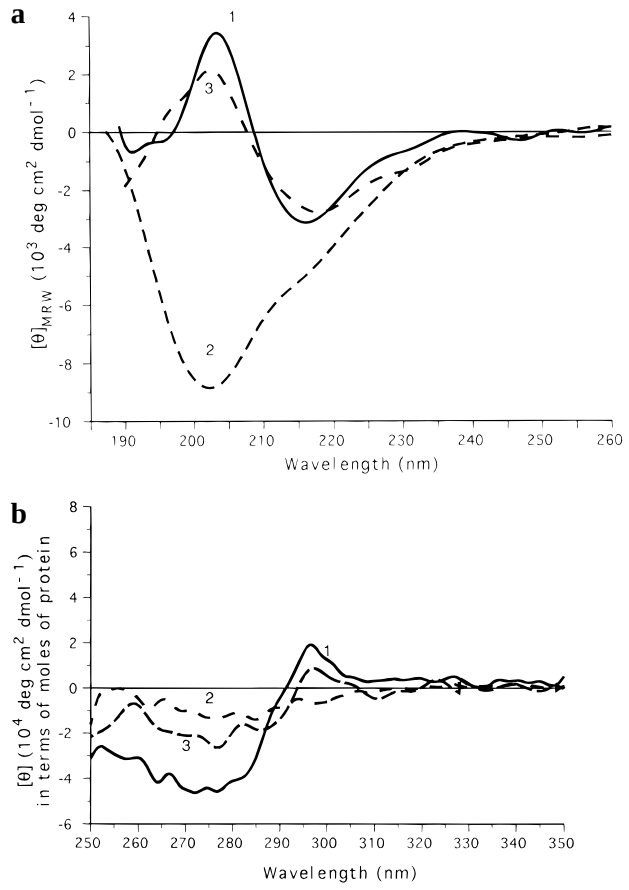

FIGURE 3: (a) Far-UV CD spectra of Fab fragments derived from 4-4-20 that are (spectrum 1) reduced and dialyzed against PBS, pH 7.4; (2) reduced and dissociated in 1 M acetic acid; and (3) reassociated in PBS. (b) Near-UV CD spectra of Fab fragments derived from 4-4-20 that are (spectrum 1) reduced and dialyzed against PBS, pH 7.4; (2) reduced and dissociated in 1 M acetic acid; and (3) reassociated in PBS.

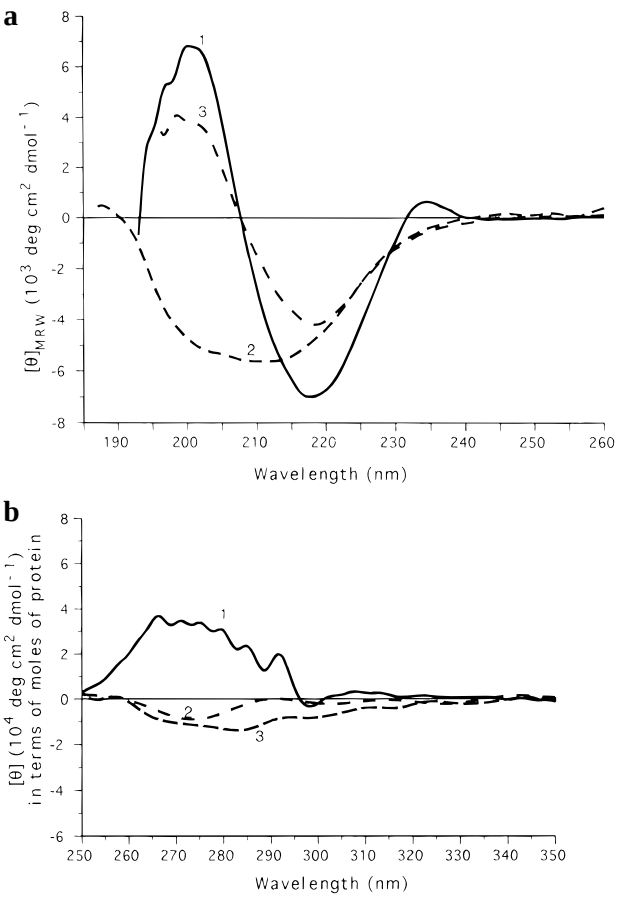

FIGURE 4: (a) Far-UV CD spectra of Fab fragments derived from NC10.14 that are (spectrum 1) reduced and dialyzed against PBS, pH 7.4; (2) reduced and dissociated in 1 M acetic acid; and (3) reassociated in PBS. (b) Near-UV CD spectra of Fab fragments derived from NC10.14 that are (spectrum 1) reduced and dialyzed against PBS, pH 7.4; (2) reduced and dissociated in 1 M acetic acid; and (3) reassociated in PBS.

of Fab 4-4-20 showed a large negative peak at 202 nm and a shoulder at 217 nm. Any measurable CD signal in the near-UV region was also lost for both Fab fragments upon dissociation of H- and L-chains. After dialysis against PBS to reassociate the L- and H-chains, the far-UV CD spectra for Fab 4-4-20 and Fab NC10.14 demonstrated significant restoration of the original CD spectrum. For the near-UV region, some restoration of the original CD spectrum was obtained for Fab 4-4-20, but Fab NC10.14 failed to show any restoration of the CD spectrum (Figures 3b and 4b).

Ligand-Complexed Fab Fragments. All three antibodies, NC6.8, NC10.8, and NC10.14, bind the sweetener ligand *N*-(*p*-cyanophenyl)-*N*′-(diphenylmethyl)guanidineacetic acid with dissociation constants of 5.3×10^{-8} M, 5×10^{-9} M, and 7.3×10^{-8} M, respectively (Anchin & Linthicum, 1993). To obtain CD spectra of the Fab−ligand complexes in the near-UV region, we maintained the concentration of the Fab fragments in the range of $(5-10) \times 10^{-6}$ M and the concentration of the ligand in the range of $(1-2) \times 10^{-5}$ M in all experiments. Based on simple calculations using the quadratic equation for the total concentrations of Fab fragments, ligand, and dissociation constants, we confirmed that more than 99% of the ligand binding sites were occupied (stoichiometrically bound) under these experimental conditions. Because the free ligand does not possess any intrinsic optical activity, all changes in CD spectra upon binding were induced by formation of the Fab−ligand complex. Expression of these CD spectral results in terms of the concentration of the bound Fab (which is essentially equal to the total Fab concentration in our experiments) allowed us to compare CD spectra of uncomplexed and ligand-complexed Fab fragments.

Figure 5a shows the near-UV CD spectra of ligand-complexed Fab fragments for all three mAb. Ligand binding altered the biphasic characteristics of the CD spectra of NC6.8 and NC10.8. For NC10.14, however, the near-UV CD spectrum of the liganded Fab changed to the negative sign. To plot the net change in CD spectra (difference spectra) for each mAb Fab fragment upon ligand binding, the CD spectra of uncomplexed Fab fragments were subtracted from the spectra of the Fab−ligand complex (Figure 5b). The difference spectra of the mAb NC10.8−ligand complex showed a broad peak with the maximum at 292 nm. The difference spectra of the NC6.8 Fab−ligand complex demonstrated a single positive maximum at 272 nm. For the NC10.14 Fab−ligand complex, the difference spectra showed two weakly resolved negative maxima around 270 and 292 nm. The difference spectra of the whole IgG−ligand complexes and Fab−ligand complexes matched very closely for all three mAb (Figure 5b).

DISCUSSION

The first studies of immunoglobulins using ORD (Jirgensons, 1969) and CD (Dorrington & Tanford, 1970) spec-

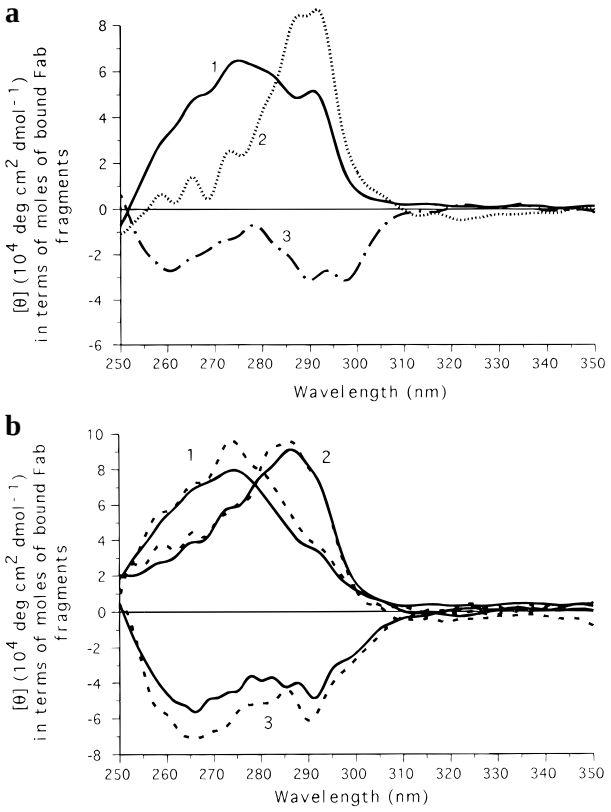

FIGURE 5: (a) Near-UV CD spectra of ligand-complexed Fab fragments derived from mAb: NC6.8 (spectrum 1); NC10.8 (2); NC10.14 (3). (b) Difference spectrum (ligand-complexed minus uncomplexed) of near-UV CD spectrum of Fab fragments (solid lines) and IgG (dashed lines) from mAb: NC6.8 (spectrum 1); NC10.8 (2); NC10.14 (3).

troscopy found that the ORD or CD spectra of homogeneous myeloma immunoglobulins and Bence-Jones proteins (L-chain dimers) always have some individual spectral details, and the overall shape and amplitude of the spectra in the far-UV region did not identify the high degree of the regular secondary structure found in these proteins by X-ray diffraction analysis (Epp et al., 1975; Poljak et al., 1973; Schiffer et al., 1973; Segal et al., 1974). The predominant β-structure in Ig domains is very consistent among all the Ig structures deposited in the Brookhaven Data Bank (Padlan, 1994). However, in many cases, including the mAb in this study, the amplitude of the far-UV CD spectra of different immunoglobulins is highly variable. For example, the amplitude of the negative portion of the CD spectrum for Fab NC10.14 in the region of 210−230 nm exceeds the amplitude of the CD spectrum of Fab 4-4-20 by more than 2-fold. Such differences are misleading in that they imply dramatic variations in the content of β-structure between the different mAb.

Azuma and co-workers (Azuma et al., 1972) were probably the first to attribute the shoulder at 230 nm in CD spectra of Bence-Jones proteins to the aromatic amino acids. The contribution of the L_a absorption band (around 220 nm) of Tyr or Phe side chains, as well as the B_b and B_a bands (225 and 200 nm, respectively) of the indole chromophore of Trp, in the origination of far-UV CD spectra was suggested in studies of several other proteins (Cosani et al., 1968; Simons & Blout, 1968) and dipeptide models (Sears & Beychok, 1970). Later, theoretical calculations (Woody, 1978, 1987) predicted that the preferred positive sign of the CD signal was derived from the coupling of L_a bands of Tyr or Phe with the immediately neighboring peptide bond chromophores, due to favorable positions of aromatic side chains around the backbone in the L-amino acid polypeptide chain. Similar analysis of Trp nearest-neighbor interactions and their contributions to the far-UV CD in the 225 nm region (B_b band) showed that either a positive or a negative sign of the CD spectra was possible (Woody, 1994). The overlap of positive chromophore bands on an essentially negative CD signal may explain the low amplitude of the CD spectra of Ig or Fab fragments near 217 nm, as well as the appearance of some spectral shoulders or peaks around 230 nm.

The CD spectra from aromatic side chains may also arise from exciton coupling of identical aromatic rings, such as Trp−Trp pairwise coupling, or coupled-oscillator interactions between different chromophore pairs, such as Trp−Tyr, Trp−Phe, or Phe−Tyr (Grishina & Woody, 1994). As we previously identified in mAb 4-4-20 (Tetin et al., 1992), many of the aromatics in the V-regions are located at the interdomain surfaces. To minimize the effects of these aromatic−aromatic interactions, it would be optimal to study the CD spectra of totally dissociated L- and H-chains of Fab fragments. However, the relatively high affinity of L- and H-chain domain interactions does not readily permit Fab dissociation in commonly used buffers, even after reduction and alkylation of the single interchain disulfide bond. When we performed a traditional procedure to achieve dissociation of reduced Fab fragments using 1 M acetic or propionic acid (Fleischman et al., 1964), as expected, the CD spectra of the dissociated protein significantly increased in amplitude in the 210−220 nm region, and were near-zero in the near-UV region. However, the spectra also turned negative in the region of 195−207 nm. Because denatured proteins and oligopeptides have a strong negative spectral peak with an amplitude higher than 2×10^4 deg cm^2 dmol^{-1} in the 190−200 nm region (Venyaminov et al., 1993), these data indicate that in addition to the elimination of the aromatic side chain effect, there was also some perturbation of the native structure. Removal of acetic acid by 48 h of dialysis against PBS reassociated the Fab fragments and reestablished the far-UV and near-UV CD spectra to a great extent in the case of Fab 4-4-20. For Fab NC10.14, however, the restoration of CD spectra was less than complete in the far-UV region, and was not achieved at all in the near-UV region. This observation suggests that the precise realignment of L and H interdomain contacts is essential in restoration of the native domain conformation. Evidently, the optimal conditions for a precise realignment for NC10.14 cannot be completely attained by simple buffer exchange. We have not measured the ligand binding affinity in the reassociated NC10.14 Fab, but reduction of affinity usually accompanies chain reassociation experiments and has been observed in experiments with several other mAb (Rinfret et al., 1985). The effects of acetic ($pK_a = 4.74$) or propionic ($pK_a = 4.87$) acid on immunoglobulin structure are not well understood, but it is likely that in the case of reduced Fab fragments, a combination of high ionic strength and a detergent-like effect of these short aliphatic acids is more important than the mere decrease of pH. Poor reassociation of L- and H-chains in the case of Fab 10.14 may be due to individual properties of this mAb and/or properties related to the λ class of the L-chain.

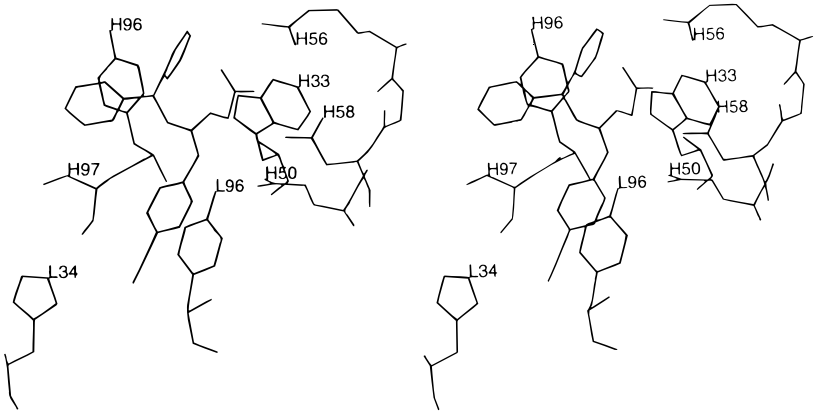

FIGURE 6: Stereoview of the contact residues in the binding site of NC6.8 Fab complexed with the guanidinium superpotent sweetener ligand (from the Brookhaven Protein Database file 2CGR). About 84% of the total surface area of the ligand is buried in the mAb binding site. One side of the ligand *p*-cyanophenyl ring is stacked against Tyr (L96), and the rings are nearly parallel. Other ligand contacts include Tyr (H96), Ser (H97), Glu (H50), Trp (H33), and Asn (H58). A salt bridge is formed between the acetic acid moiety and Arg (H56). The induced near-UV CD spectra for the NC6.8−ligand complex are predicted to be due to ligand interaction with Tyr (L96).

Ligand binding induced pronounced changes in the near-UV CD spectra for all three mAb studied here. The ligand induced positive CD peaks in the 260−300 nm range for both NC6.8 and NC10.8 Fab fragments, but the opposite sign of the CD spectrum was observed for Fab NC10.14. The ligand used in the present study does not possess any endogenous optical activity. Thus, all changes in the CD spectra of antibody−ligand complexes can be assigned as spectral perturbations induced by the binding of the ligand. The induced CD spectrum around 295 nm can be unambiguously assigned to the L_b electronic transition of Trp, as it has the lowest energy absorption band among protein chromophores. The broad absorption band in the region 260−287 nm may be caused by a strong L_a transition of Trp or a weaker L_b transition of the Tyr. The longest wavelength at which we expect a contribution of the Phe L_b band is 268 nm, but its intensity is more than 8 times lower than the Tyr absorption at the same wavelength (Strickland, 1974). Theoretically, there may also be a contribution of an induced CD originating from the *p*-cyanophenyl portion of the ligand at the short-wavelength edge of the NC6.8 and NC10.14 spectra. Nevertheless, the dominant role of intrinsic mAb chromophores in the origination of the induced CD spectra for the entire region of 260−300 nm has also been demonstrated by fluorescence polarization spectra in which the bound ligand greatly increases polarization throughout the excitation spectra for all three mAb studied here (Tetin and Linthicum, unpublished results).

The near-UV CD spectra of the mAb−ligand complexes in this study have the shape of Trp and/or Tyr absorption bands, and according to Strickland (1974), these types of spectra are indicative of nongenerate exciton $\mu-\mu$ coupling. The near-UV transitions of the aromatic side chains have a tendency to couple most strongly with the far-UV transitions of other aromatic side chains, peptide chromophore, or electronic transitions of prosthetic groups, such as bound ligands. The distance for such interactions is assumed to be within the range of 10−15 Å (Strickland, 1974). Theoretically, the highest amplitude of the induced CD signal is obtained when two aromatic rings are parallel (the line connected to their centers is normal to both of them) and the vectors of coupling transitions are displaced by a 45° angle (Grishina and Woody, 1994).

The three-dimensional structures of NC6.8 Fab fragments have been solved at high resolution for the uncomplexed (2.7 Å) and ligand-complexed (2.2 Å) forms (Guddat et al., 1994). The ligand makes several contacts with H- and L-chain residues in the binding site as shown in Figure 6. The Tyr at position L:96 of the L-chain (located in the third CDR) interacts with the *p*-cyanophenyl ring of the ligand. The distance between these rings is less than 4 Å, while the angle between their planes is only 11° and they are rotated along their axes by 9° (Figure 6). The arrangement of the *p*-cyanophenyl moiety of the ligand and the contact residue Tyr L:96 appears to fulfill the requirements for the induction of the CD band. In the crystal structure, ligand binding did not to alter the local environments of aromatics in the V-regions that were not associated with the ligand.

The binding site of mAb NC10.8 has been characterized using a combination of site-directed mutagenesis, photoaffinity ligand labeling, fluorescence, and absorption spectroscopy (Anchin et al., 1994a,b). Based on these data, L:96W is in contact with the ligand. Using a theoretical molecular model of the binding site, it has been proposed that there is a planar contact between Trp L:96 and the *p*-cyanophenyl portion of the ligand (Anchin et al., 1994a,b). The difference CD spectra for the ligand-complexed NC10.8 Fab identify the L_b absorption band (maximum at 293 nm) of the Trp chromophore. Thus, the CD data presented herein support the proposed model of the NC10.8 binding site.

Antibody NC10.14 has four Trp (H:52, H:53, L:91, and L:96) in the H- and L-chain CDR (Anchin & Linthicum, 1993). The crystallographic studies of the NC10.14 Fab−ligand complex have been completed (2.6 Å resolution, *R*-value 0.194), and the coordinates are currently undergoing final refinements (Gudatt et al., unpublished results). Preliminary examination of this structure shows the ligand to be wedged between L:91W and a Tyr at H:100k. We propose that the two peaks observed for the NC10.14 Fab−ligand complex difference spectra originate from the L_b absorption band (maximum at 293 nm) of the Trp chromophore at L:91 and the L_b absorption band (maximum at 270 nm) of Tyr at H:100k. Further inspection of refined crystallographic data and site-directed mutagenesis experiments underway should support or correct these predictions.

CD is a popular and powerful tool for the study of antibody structure. However, the contribution of aromatic side chain chromophores to the CD spectra should not be overlooked in the analysis of antibodies, their fragments, and recombinant molecules. The location of Tyr or Trp in the binding site may identify important geometric arrangements of antigen and contact sites. In the case of the anti-fluorescein antibody 4-4-20, the aromatic residues induce CD in the bound ligand (Tetin et al., 1992). For the anti-guanidinium sweetener mAb studied here, the *p*-cyanophenyl moiety of the ligand acts as a "molecular pointer", and the induced CD spectra identify the specific aromatic side chain contacts. The *p*-cyanophenyl portion of the ligand is known to make a significant contribution ot the sweetness potency of this family of ligands (DuBois et al., 1993; Muller et al., 1992). The study of these mAb−ligand complexes may help to understand the stereochemical properties of these superpotent sweeteners and their interactions with putative sweet taste binding sites.

ACKNOWLEDGMENT

We thank Prof. R. W. Woody for his insight and helpful suggestions regarding this work. We also thank Prof. F. Schroeder for permitting us to use his Jasco-710 instrument for these studies; his discussions were greatly appreciated.

REFERENCES

Anchin, J. M., & Linthicum, D. S. (1993) *Mol. Immunol. 30*, 1463−1471.

Anchin, J. M., Droupadi, P. R., DuBois, G. E., Kellogg, M. S., Nagarajan, S., Carter, J. S., & Linthicum, D. S. (1994a) *J. Immunol. 153*, 3059−3069.

Anchin, J. M., Mandal, C., Culberson, C., Subramaniam, S., & Linthicum, D. S. (1994b) *J. Mol. Graphics 12*, 257−266.

Azuma, T., Hamaguchi, K., & Migita, S. (1972) *J. Biochem. 72*, 1457−1467.

Cosani, A., Peggion, E., Verdini, A. S., & Terbojevichi, M. (1968) *Biopolymers 6*, 963−971.

Dorrington, K. J., & Tanford, C. (1970) *Adv. Immunol. 12*, 333−381.

Droupadi, P. R., & Linthicum, D. S. (1995) *Int. J. Biochem. Cell Biol. 27*, 351−357.

DuBois, G. E., Walters, D. E., & Kellogg, M. S. (1993) in *Flavor measurement* (Ho, C.-T., & Manley, C. H., Eds.) pp 239−266, Marcel Dekker, New York.

Epp, O., Lattman, E. E., Schiffer, M., Huber, R., & Palm, W. (1975) *Biochemistry 14*, 4943−4952.

Fleischman, J. B., Porter, R. R., & Press, E. M. (1964) *Biochem. J. 88*, 220−228.

Grishina, I. B., & Woody, R. W. (1994) *Faraday Discuss. 99*, 1−18.

Guddat, L., Shan, L., Anchin, J., Linthicum, D. S., & Edmundson, A. B. (1994) *J. Mol. Biol. 236*, 247−274.

Herron, J. N., He, X., Mason, M. L., Voss, E. W., & Edmundson, A. B. (1989) *Proteins: Struct., Funct., Genet. 5*, 271−280.

Jirgensons, B. (1969) *Optical Rotatory Dispersion of Proteins and Other Macromolecules*, pp 96−100, Springer-Verlag, New York.

Kabat, E. A., Wu, T. T., Perry, H. M., Gottesman, K. S., & Foeller, C. (1991) U. S. Department of Health and Human Services, NIH Publication No. 91−3242.

Kranz, D., & Voss, E. W., Jr. (1981) *Mol. Immunol. 18*, 889−898.

Mach, H., Middaugh, C. R., & Lewis, R. V. (1992) *Anal. Biochem. 200*, 74−80.

Muller, G. W., Walters, D. E., & DuBois, G. E. (1992) *J. Med. Chem. 35*, 740−743.

Padlan, E. A. (1990) *Proteins*: *Struct., Funct., Genet. 7*, 112−124.

Padlan, E. A. (1994) *Mol. Immunol. 31*, 169−217.

Poljak, R. J., Amzel, L. M., Chen, B. L., Phizackerley, R. P., & Saul, F. (1973) *Proc. Natl. Acad. Sci. U.S.A. 70*, 3305−3310.

Rinfret, A., Horne, C., Dorrington, K. J., & Klien, M. (1985) *J. Immunol. 135*, 2574−2581.

Schiffer, M., Girling, R. L., Ely, K. R., & Edmundson, A. B. (1973) *Biochemistry 12*, 4620−4631.

Sears, D. W., & Beychok, S. (1970) *Physical Principles and Techniques of Protein Chemistry* (Leach, S. J., Ed.) Part C, pp 445−593, Academic Press, New York.

Segal, D. M., Padlan, E. A., Cohen, G. H., Rudikoff, S., Potter, M., & Davies, D. R. (1974) *Proc. Natl. Acad. Sci. U.S.A. 71*, 4298−4302.

Simons, E. R., & Blout, E. R. (1968) *J. Biol. Chem. 23*, 218−221.

Strickland, E. H. (1974) *CRC Crit. Rev. Biochem. 2*, 113−175.

Tetin, S. Y., Mantulin, W. W., Denzin, L. K., Weidner, K. M., & Voss, E. W., Jr. (1992) *Biochemistry 31*, 12029−12034.

Venyaminov, S. Y., Balikalov, I. A., Shen, Z. M., Wu, C.-S. C., & Yang, J. T. (1993) *Anal. Biochem. 214*, 17−24.

Woody, R. W. (1978) *Biopolymers 17*, 1451−1467.

Woody, R. W. (1987) *Proc. Fed. Eur. Chem. Soc. Second Int. Conf. CD (Budapest)* (Kajtar, M., Ed.) pp 38−56, VCH Publishers, New York.

Woody, R. W. (1994) *Eur. Biophys. J. 23*, 253−262.

BI951576H